

Editorial Manager(tm) for Journal of Computational Neuroscience  
Manuscript Draft

Manuscript Number: JCNS266R2

Title: Oscillations and slow patterning in the antennal lobe

Article Type: Regular Article

Section/Category:

Keywords: Olfactory; Insect; Synchrony; Odor; Model

Corresponding Author: Dr. Ehud Sivan, PhD

Corresponding Author's Institution: Boston University

First Author: Ehud Sivan, PhD

Order of Authors: Ehud Sivan, PhD; Nancy Kopell, PhD

Manuscript Region of Origin:

**Abstract:** Odor presentation generates both fast oscillations and slow patterning in the spiking activity of the projection neurons (PNs) in the antennal lobe (AL) of locusts, moths and bees. Experimental results indicate that the oscillations are the result of the interaction between the PNs and the inhibitory local neurons (LNs) in the AL; e.g., blocking inhibition by application of GABA-receptor antagonists abolishes these oscillations. The slow patterning, on the other hand, was shown to be somewhat resistant to such blockage. In a H-H model, we reproduce both the oscillations and the slow patterning. As previously suggested, the oscillations are the result of the interaction between the PNs and LNs. We suggest that calcium and calcium-dependent potassium channels (found in PNs of bees and moths) are sufficient to account for the slow patterning resistant to the application of GABA-receptor antagonists. The intrinsic bursting property of the PNs, resulting from these additional modeled currents, give rise to another network feature that was seen experimentally in locusts: a relatively small increase in the number of additional generated PN action potentials when LN input is blocked. Consequently, the major effect of network inhibition is to redistribute the action potentials of the PNs from bursting to one action potential per cycle of the oscillations.

Friday, August 05, 2005

To Whom It May Concern:

Enclosed is our manuscript, "Oscillations and slow patterning in the antennal lobe", which we wish to submit for publication in The Journal of Computational Neuroscience as a regular article.

Thank you for your attention,  
Ehud Sivan and Nancy Kopell

PS. Please see our comments regarding action editors and reviewers in the Comments section.

**“I had a lot of difficulties understanding what was done in Figure 5 and what it was supposed to prove.”**

In figure 5 we quantified the similarity of the slow patterning in the PN activity with and without inhibition. As the activity of each PN is not identical in different trials of the same network configuration, we computed the firing probabilities of the PNs in 100 ms bins along the simulation for each configuration (10 trials each). The difference between the firing probabilities of different PNs (or different network configurations) represents the difference in the slow patterning of the PNs (i.e., PNs that tend to fire at the same times during the simulation have small differences in their firing probabilities). Thus, by subtracting the firing probabilities of different PNs (and the same PN at different configuration) we look at the absolute difference between the activities of the PNs.

We think this method is more intuitive than other clustering methods used to find the relative resemblance of n-dimensional vectors. Moreover, it provides a bin by bin comparison of the behavior of the PNs and therefore better describes the differences in their slow patterning. We added, however, an inset to Fig. 5 where we use the traditional hierarchical clustering and get similar results.

To clarify what we did in Figure 5 we have rewritten its legend, as well as the relevant text (p. 9).

**“I also discovered a set of honeybee AL modeling papers that have been omitted in the citations, and that deal with mechanisms of oscillations in the AL.”**

We searched the literature again but could not find the papers mentioned and therefore we did not add new references.

## Oscillations and slow patterning in the antennal lobe

Ehud Sivan & Nancy Kopell

*Center for Biodynamic, Boston University, 111 Cummington Street Boston, MA 02215, USA.*

**Corresponding author:** Ehud Sivan, Center for Biodynamic, Boston University, 111

Cummington Street Boston, MA 02215, USA, 617-353-1487, 617-353-4889 (F),

[ehud@bu.edu](mailto:ehud@bu.edu).

## **Abstract**

**Odor presentation generates both fast oscillations and slow patterning in the spiking activity of the projection neurons (PNs) in the antennal lobe (AL) of locusts, moths and bees. Experimental results indicate that the oscillations are the result of the interaction between the PNs and the inhibitory local neurons (LNs) in the AL; e.g., blocking inhibition by application of GABA-receptor antagonists abolishes these oscillations. The slow patterning, on the other hand, was shown to be somewhat resistant to such blockage. In a H-H model, we reproduce both the oscillations and the slow patterning. As previously suggested, the oscillations are the result of the interaction between the PNs and LNs. We suggest that calcium and calcium-dependent potassium channels (found in PNs of bees and moths) are sufficient to account for the slow patterning resistant to the application of GABA-receptor antagonists. The intrinsic bursting property of the PNs, resulting from these additional modeled currents, give rise to another network feature that was seen experimentally in locusts: a relatively small increase in the number of additional generated PN action potentials when LN input is blocked. Consequently, the major effect of network inhibition is to redistribute the action potentials of the PNs from bursting to one action potential per cycle of the oscillations.**

Keywords: Olfactory, Insect, Synchrony, Odor, Model.

## Introduction

The antennal lobe (AL), the first relay of the insect olfactory system, is a network of excitatory projection neurons (PNs) and inhibitory local neurons (LNs) ([Laurent, 1996](#); [Hansson and Anton, 2000](#)). Odor presentation was shown to evoke complex temporal patterns of firing activity in the PNs there ([Christensen et al., 2003](#); [Stopfer et al., 1997](#); [Laurent and Davidowitz, 1994](#)). In some species (e.g. honeybees and locusts) these patterns may consist of alternating epochs of high-frequency firing and quiescence where each epoch may last up to a few hundred milliseconds. Different odors can evoke different temporal patterns in one PN, and one odor can evoke different patterns in simultaneously recorded PNs. These patterns are consistent across trials ([Laurent and Davidowitz, 1994](#); [Wehr and Laurent, 1996](#); [Laurent et al., 1996](#)). In others (e.g. moths) it may consist of prolonged bursting where the bursting characteristics change over time followed by a prolonged quiescence epoch ([Christensen et al., 2003](#)).

The origin of this slow patterning is unknown: Wehr and Laurent ([1999](#)) showed that, in locusts, the input to the AL shows no such patterning. Also, application of the GABA-receptor antagonists, picrotoxin and bicuculline, to the AL leads to either no change in the slow patterning ([Stopfer et al., 1997](#); [MacLeod and Laurent, 1996](#); [MacLeod et al., 1998](#)) or a change in slow patterning characteristics ([Christensen et al., 1998](#); [Sachse and Galizia, 2002](#)) but does not eliminate the slow patterning phenomenon. Bazhenov et al. ([2001a](#); [2001b](#)) suggested that the origin of the slow patterning in locust is a strong and slow inhibition of PNs by LNs that is insensitive to picrotoxin. However, no such inhibition has yet been found.

Odor presentation was also shown to evoke high frequency oscillations (20 Hz – 35 Hz) ([Stopfer et al., 1997](#); [Laurent and Naraghi, 1994](#); [Heinbockel et al., 1998](#)). It was suggested that these oscillations are the result of the interaction between the excitatory PNs and the inhibitory LNs in the AL, since application of picrotoxin abolishes these

oscillations ([Stopfer et al., 1997](#); [MacLeod and Laurent, 1996](#)). Such oscillations have been found in locusts ([Laurent and Naraghi, 1994](#)), moths ([Heinbockel et al., 1998](#)) and bees ([Stopfer et al., 1997](#)). Moreover, similar oscillations have been seen in the olfactory bulb (OB) of vertebrates ([Adrian, 1942](#); [Bressler and Freeman, 1980](#); [Friedrich and Laurent, 2001](#); [Kay, 2003](#)), which is believed to be an analogue to the insect AL ([Laurent et al., 2001](#)).

Theoretical work on networks of excitatory and inhibitory networks in general ([Whittington et al., 2000](#); [Tiesinga et al., 2001](#); [Borgers and Kopell, 2003](#)), and more specific networks constructed to capture either the known connectivity in the AL/OB ([Ermentrout et al., 1998](#)), the known internal properties of the neurons in the AL/OB ([Bazhenov et al., 2001a](#); [2001b](#)) and/or the known morphological structure of the neurons in the AL/OB ([Davison et al., 2003](#)) each shows that such networks are capable of producing oscillatory behavior at frequency ranges that are similar to the one observed experimentally. However, only Bazhenov et al. ([2001a](#); [2001b](#)) reproduced the slow patterning as well as the observed oscillations. In their modeling they assumed the existence of calcium and calcium-dependent potassium channels in the LNs and modeled these neurons to be non-spiking (as was observed experimentally in the locust; [Laurent, 1996](#)). Bazhenov et al. ([2001a](#); [2001b](#)) also assumed a random connectivity between the various neurons in the AL and, as mentioned above, incorporated a strong and slow picrotoxin-insensitive inhibition of PNs by LNs.

As in Bazhenov et al. ([2001a](#); [2001b](#)) we also aim to capture these two phenomena, but with somewhat different assumptions. We do not assume any slow inhibition; rather, we suggest a mechanism for the observed slow patterning that is based upon the internal calcium concentration of the PNs: Calcium concentration is a good candidate for generating slow changes in neuron activity as its removal rate can be hundreds of milliseconds ([Av-Ron et al., 1993](#)) and it can indirectly affect the threshold

of the neuron (and hence its firing rate) through calcium-dependent ion channels (e.g., calcium-dependent potassium channels; [Av-Ron et al., 1993](#)). Moreover, calcium and calcium-dependent potassium channels were found in the PNs of moths ([Mercer and Hildebrand, 2002a; 2002b](#)) and bees ([Grunewald, 2003](#)). Thus, we incorporate calcium and calcium-dependent potassium channels for the PNs (we further address this decision in the Discussion).

The connectivity between the various cells in our model is also different from the random connectivity suggested by Bazhenov et al. ([2001a; 2001b](#)): we assume an all-to-all connectivity between the PN and LN cells as well as among the LNs (This is not crucial, however, and a network with sparser connectivity, as low as 70% connectivity probability, was also simulated with similar results; data not shown). Notice that we assume no connectivity among the PNs.

We start by showing that our model replicates experimental data: (i) the observed oscillations in the AL activity during odor presentation ([Laurent and Naraghi, 1994](#)). (ii) The abolition of the oscillation when applying GABA-receptor antagonists ([MacLeod and Laurent, 1996](#)) (simulated in our model by completely blocking the LN activity). (iii) The slow patterning in the spiking activity of the PNs ([Wehr and Laurent, 1999](#)). (iv) The persistence of this patterning even when LN input is blocked ([MacLeod and Laurent, 1996; MacLeod et al., 1998; Stopfer et al., 1997](#)). We then analyze the model, in order to understand the mechanisms responsible for the observed experimental data.

## **Methods**

### Interneurons model

For the PNs and LNs we considered a single compartment model that includes voltage- and calcium-dependent currents described by Hodgkin-Huxley kinetics ([1952](#)). A full

description of this model and of the model used for the synapses between the neurons is given in the Appendix.

### Network geometry and stimulation

The model network consists of 14 identical PNs and 5 identical LNs (which differ only in their random initial condition), thus keeping the ratio between the number of PNs and LNs in the locust (830 and 330 respectively; [Leitch and Laurent, 1996](#)). We chose 14 PNs to simulate the activity of the average “Functional Subset” (FS) that was hypothesized to exist in insects ([Sivan and Kopell, 2004](#); [Kay, 2004](#)). The network connectivity is simple: Within each FS, each PN excites all the LNs and each LN inhibits all the PNs as well as the other LNs. (This all-to-all connectivity may be sparser between FSs.) The inhibitory synapses of the LNs are graded synapses, since the LNs are non-spiking ([Laurent, 1996](#)). In our model the PNs do not excite one another.

Each neuron in the network gets input from 60-120 ORNs converging on a single glomerulus ([Laurent, 1996](#)) where the exact number was chosen randomly for each glomerulus. Each neuron was connected to a different glomerulus. Although, in the locust, each PN is connected to more than 1 glomerulus (10 to 20 glomeruli; [Laurent, 1996](#)), we decided to simulate input only from a single glomerulus to simplify the simulation and because, in other species with large glomeruli, each PN is connected to a single glomerulus ([Hansson and Anton, 2000](#)).

We simulated the activity of each ORN by a Poisson distribution of action potentials (following Bazhenov et al., [2001a](#); [2001b](#)): Each ORN had a firing rate at rest and another firing rate when an odor was presented; the latter could be higher, lower or equal to the resting firing rate. We set the resting firing rate to be between 15-25 Hz (in line with [de Bruyne et al., 2001](#)), 50-150 Hz the higher firing rate (in line with Bazhenov et al., [2001a](#); [2001b](#)), and 0 Hz the lower firing rate. When an odor was introduced, each ORN changed its firing rate gradually to its odor-related firing rate.

When the odor was removed each ORN gradually returned to its resting firing rate. Both changes in firing rate (introduction and removal of odor) followed the following equation:

$$\lambda(t) = \lambda_{start} + (\lambda_{end} - \lambda_{start}) \cdot \left( \frac{\tanh\left(\frac{(t - t_{event})}{change\_rate/3} - 3\right) + 1}{2} \right), \quad (1)$$

where  $\lambda_{start}$  and  $\lambda_{end}$  are the start and end firing rates respectively,  $t_{event}$  is the time the odor was introduced/removed and  $change\_rate$  is the change time constant. For each ORN, we set  $change\_rate$  to be between 50 ms and 500 ms for odor introduction and between 400 ms and 2000 ms for odor removal (in line with [Wehr and Laurent, 1999](#)). All ORNs connected to the same glomeruli had the same rest firing rate, odor firing rate, and odor introduction/removal change rates based on the assumption that all ORNs converging on the same glomerulus express the same receptor type ([Laurent et al., 2001](#)) and thus behave the same. Consequently, the noise in the input results from the different times each ORN fires its action potentials during the simulation.

Odor introduction lasted one second and increased the firing rate of ORNs connected to 12 glomeruli and lowered the firing rate of ORNs connected to the remaining two glomeruli as suggested theoretically ([Sivan and Kopell, 2004](#)), and seen experimentally ([Shields, 2001](#)).

We simulated odor repetition by rerunning the simulation with the same interneurons connected to the same glomeruli, and in the repeated simulation each ORN exhibited the same resting, changing (i.e.,  $change\_rate$ ) and odor firing rates. However, the exact time each ORN fired an action potential changed with each trial.

## Results

### The PNs exhibit slow patterning

We simulated 10 trials of odor presentations to the network; Fig. 1 depicts the firing activity of 10 PNs (out of the 14 PNs) during the first 4.5 secs of the simulation. The grey area represents the 1 sec odor presentation. As can be seen, the simulated PNs exhibit slow patterning. In particular:

1. There are epochs of higher and lower firing rates.
2. The epochs are quite consistent between odor repetitions
3. During the odor presentation some PNs are inhibited by the odor (i.e., lower their firing rate; e.g., PN 12) and some are excited by it (i.e., increase their firing rate; e.g., PN 3).
4. The effect of the odor extends beyond the odor presentation.
5. Different PNs start responding at different times to the odor (e.g. PN 4 and PN 9).

### The network shows ~20 Hz oscillations

The model LFP, seen in Fig. 2A, is the sum of all synaptic conductances activated by the action potentials of all PNs (see [Sivan and Kopell, 2004](#) for details). As can be seen in Fig 2B, the power spectrum of the LFP has a peak close to 20 Hz.

### The slow patterning is preserved even when the inhibition from the LNs is blocked; the oscillations are not.

To check the affect of the LNs on the activity of the PNs we simulated an additional 10 odor presentations to the network while completely blocking the inhibitory synapses, thus isolating the PNs (which do not excite one another). Fig. 3 shows the firing activity of the same 10 PNs as in Fig. 1. As can be seen, there is qualitative similarity between the first 10 trials (lower stripe in each PN) and the last 10. Fig 4 shows a close up on the

membrane potential of one PN in two trials, with (Fig. 4A) and without (Fig. 4B) inhibition from the LNs: as observed experimentally, the number of action potentials and the overall behavior remain similar (compare Fig. 4 to Fig. 2 in [MacLeod and Laurent, 1996](#)).

Figure 5 shows the firing probability of each PN in 100 ms bins along the two seconds of simulation after the odor is presented. Looking at the difference between the activity of the same PN with and without inhibition (represented by the diagonal in the table in Fig. 5) we see that all PNs have almost the same firing probability with and without inhibition. Moreover, except the last bin in PN 7, the difference in firing probability never exceeds 50% in any bin. By contrast, when comparing the activity of different PNs (represented by the other entries in the table in Fig. 5), we see that the firing probability in most bins differ, and in many cases with probability far greater than 50%. Moreover, any two PNs have at least one bin where the difference in firing probability is higher than 50%.

We thus conclude that, in the simulation, the slow patterning is preserved even when the inhibition is blocked. The synchronization between the PNs, on the other hand, is lost without the input from the LNs, as can be seen in the relatively flat power spectrum of the LFP (compare Fig. 2C with Fig. 2B).

This result is independent of the non-spiking characteristic of the LNs. Fig 6 shows the result of a simulation in which we changed the LNs to be spiking. The figure shows the existence and similarity of slow patterning with and without inhibition (Fig. 6A), and that LFP oscillations exist only in the presence of LN inhibition (compare left and right panels of Fig. 6B).

The temporal activity of the PNs in the moth, *Manduca sexta*, is described to be multiphasic rather than exhibiting slow patterning ([Christensen et al., 2003](#)). The PNs

start firing a burst of action potentials  $\sim 100$  ms after odor presentation and the properties of this burst change in time. Three different phases were identified in this burst; in the first phase the action potentials are very rapid ( $> 150$  Hz) and the LFP shows very high amplitude without LFP oscillations. In the next phase LFP oscillations are formed while the PNs continue to fire at frequencies up to 3 times higher than the oscillation rate, and the action potentials seem not to be locked to the LFP oscillations. The last phase occurs once the odor presentation stops; the PNs continue to fire at high frequencies for a while and the LFP oscillations are considerably reduced. We simulated this activity by using the exact same network as in Fig. 6 but increasing and synchronising the input to the PNs from the ORN cells. We were able to qualitatively obtain the three phases (compare Fig. 7 to Fig. 1, [Christensen et al., 2003](#)). This suggests that the slow patterning and multiphasic responses may be two activity modes of the same network in which only the input properties vary.

The slow patterning in the simulation is the result of the input and the internal calcium concentration in the PNs

A typical stand alone activity of a PN connected to an excited glomerulus is seen in Fig. 4B. As can be seen, the PN generates a burst of action potentials (marked by an arrow) shortly after the odor is presented. This burst is followed by a somewhat prolonged quiescent period, which is followed by alternating periods of firing and quiescence that last beyond the termination of the odor presentation. These alternating periods are followed by a quiescent period (marked by the arrow head) that is followed by the recovery of the PN to its normal firing rate. As can be seen in Fig. 3 and Fig. 4A, this firing pattern is quite consistent between trials, whether or not the PN is connected to the rest of the network.

A close look at the input onset to the PN (Fig. 4C) reveals the reason for the late onset of the initial burst: Although the odor is presented at 1000 ms, it takes the ORNs

time to react (because of the odor presentation rate; see Methods); once enough of them start to fire, the PN is activated. During this initial burst, calcium enters the PNs through voltage-dependent calcium channels (Fig. 4D). The calcium causes the activation of calcium-dependent potassium channels, which eventually ends this initial burst. From this point, as long as the odor presentation continues, the two opposing forces (the excitation from the input and the inhibition from the calcium-dependent potassium channels) determine the behavior of the PN; following the periodic solution of the underlying equations, the cell either fires periodic single action potentials or periodic short bursts. Also, since the input is somewhat noisy (see Fig. 4C), the period length may differ and the cell might even switch between bursting and firing a single action potential. Since both the calcium and the odor have long removal rates this behavior continues beyond the odor presentation (see Fig. 4B). Since the calcium removal rate is longer than the odor removal rate, the alternations are followed by a long quiescent period (marked by the arrow head in Fig 4B) that lasts until the internal calcium concentration resumes its normal level (see Fig. 4B and 4D). This typical behavior differs in details among PNs because of the difference in their related ORN input.

A step current injection alone cannot generate the slow patterning. When introducing such a stimulus in the simulation, the PN fires only an initial burst followed by a train of spikes as long as the injection continues (data not shown). Thus we conclude that the combination of the input shape and of the intrinsic properties of the PNs generates the slow patterning in the simulation. This initial burst was not seen experimentally in locusts ([Wehr and Laurent, 1999](#)); we further address this issue in the Discussion.

The LN redistribute and synchronize the activity of the PNs, thus creating the oscillations in the LFP

There are two questions regarding the dynamics of the network. (i) How does the network generate synchronized oscillations? (ii) How can the network produce such high frequency oscillations ( $> 20$  Hz) when the internal bursting frequency of its excitatory neurons is less than 20 Hz (even PN 3 with the highest firing frequency, seen in Fig. 3, has less than 20 Hz firing frequency)?

The answers lie in the activity of the LNs which have the following effects on the activity of the PNs:

1. *The LNs synchronize the internal burst activity of all the PNs, to give rise to oscillations in the LFP.* This phenomenon is essentially the same as reported in other models of the gamma oscillations ([Whittington et al., 2000](#); [Tiesinga et al., 2001](#); [Borgers and Kopell, 2003](#); [Kopell et al., 2000](#)). The excitatory cells are temporarily suppressed by the inhibition; since the excitatory cells integrate inhibition from many of the inhibitory cells they can be much more synchronous than the first set of inhibitory spikes. The more synchronous spikes from the excitatory cells then synchronize the inhibitory ones. In the absence of noise and heterogeneity complete synchrony can happen in one cycle ([Borgers and Kopell, 2003](#)). When there is noise and heterogeneity, as in the current situation, approximate synchrony happens in one or two cycles ([Borgers and Kopell, 2003](#)). The abrupt initiation of the external input (resulting from the odor presentation) makes the synchrony happen even faster than would occur by self-organization.
2. *The LNs redistribute the firing pattern of each PN such that a PN fires usually one or two action potentials in each of its internal bursts.* The short synaptic delay between the PNs and LNs (2 ms, simulating the dendro-dendritic synapses seen in the OB of mice; [Hinds and Hinds, 1976](#)) causes the inhibition of the LNs onto the

PNs to arrive in the midst of the PN internal burst (at least in the highly activated PNs). Consequently, these PNs stop their burst in the middle, and resume it once the LN inhibition wears off. The drive needed to resume the internal burst is the result of the relatively low calcium concentration the cell reaches after firing only a partial burst. Thus, instead of firing bursts of three or more action potentials, these PNs now fire one or two action potentials at the frequency defined by the LN inhibition (compare Fig. 8A & 8B; the underlying LFP oscillations are readily seen in the membrane potential activity in Fig. 8B).

3. *The PNs do not fire in each of the underlying network oscillations and therefore maintain their lower-than-LFP-oscillations firing frequency.* As can be seen in Fig. 8A, some internal PN bursts contain only one or two action potentials. In those bursts, once the PN fires its action potentials, it does not resume firing until the time of its next intrinsic burst (as determined by its  $< 20$  Hz bursting rate). Consequently, even when the inhibition of the LNs wears off, the PN does not fire, causing the PN to miss a cycle or two (Seen in the sub-threshold membrane activity in Fig. 8B). Its next bursting, however, will be synchronized to the overall oscillations, since it will not be able to fire during LN inhibition periods.
4. *The length of the LN inhibition onto the PNs determines the frequency of the LFP oscillations.* As observed experimentally and theoretically ([Traub et al., 1996](#); [Wang and Buzsaki, 1996](#); [Borgers and Kopell, 2003](#)), the time course of the inhibitory synapse onto the excitatory cell dictates the length of the quiescent period and thus the duration of the oscillation; in this network this is also the case.

## Discussion

In this paper we showed that the interaction between the LNs and PNs is sufficient to generate the oscillations seen in the LFP. The role of the LNs is to redistribute the

action potentials of the PNs and thus to synchronize them with the underlying network oscillations. We also showed that the input shape to the PNs, together with the calcium and calcium dependent potassium channels found in the PNs (reported in moths (Mercer and Hildebrand, [2002a](#); [2002b](#)) and bees ([Grunewald, 2003](#))), can account for the slow patterning insensitive to application of GABA-receptor antagonists.

Our study is compatible with the idea that network activity also contributes to the observed slow patterning in the AL. Some of the slow patterning observed is not easily reproduced in our model (e.g., strong hyperpolarization followed by enhanced firing of the PNs, as seen in Fig. 2A, [Stopfer et al, 2003](#)). Moreover, we do not claim that GABA-receptor antagonists block all network inhibition in the AL; there have been several papers suggesting that picrotoxin does not block all network inhibition ([Sachse and Galizia, 2002](#); [Christensen et al., 1998a](#)) and that there is more than one type of inhibitory synapse in the AL ([Christensen et al., 1998b](#); [Stopfer et al., 1997](#)). What we suggest is another mechanism responsible for the observed slow patterning, based on calcium and calcium-dependent potassium channels, which coexists along with the network inhibition. What we show is that this mechanism can explain a variety of slow patterning features (see Fig. 3) that were reported to be resistant to application of GABA-receptor antagonists. Therefore, we argue that the strong and slow network inhibition suggested by Bazhenov et al. ([2001a](#), [2001b](#)), is not required.

The initial burst that the simulated PN fires in response to a step current injection was not reported in experimental current injections to the PNs of locust ([Wehr and Laurent, 1999](#)). We were able to reproduce the experimental results (i.e., no initial burst) in our model when we changed the PN parameter and assumed that the level of calcium in the cell is very low prior to the current injection (this might be the case if the cell was deprived of input before the injection). These results, however, were not robust

over a wide range of injection levels. We note that the currents in the locust PN are not fully known, and may differ from those used in our model.

That slow patterning exists in many species, perhaps using different mechanisms, suggests that this phenomenon is important for the organism and is not a by-product. Indeed, it was suggested that the slow patterning may help decorrelate the PN activity and thus make activity of KCs (which are connected to the PNs and rely on their coincident activity) more sparse ([Laurent, 2002](#)). Another previous idea was that it codes odor temporal information such as time of odor onset, offset and intensity change as well as odor duration ([Christensen et al., 2003](#); [Sivan and Kopell, 2004](#)). We suggest that the slow patterning may also facilitate the grouping of activity of PNs that belong to the same odor source in a multi-source environment. That is, under normal conditions, at any given time, the insect is exposed to a number of odors, where each odor-source may activate a combination of PNs. Under these conditions, slow patterning in the activity of the PNs may ensure that PNs activated by different odors will not coincide in their temporal activity and thus the insect will be able to distinguish between different odors. A similar idea was proposed for the adaptation in the mitral cells in the OB ([Wilson and Stevenson, 2003](#)), and indeed the slow patterning may be regarded as a type of adaptation.

## **Acknowledgements**

We thank Mark Stopfer for discussions and valuable comments. This work was supported by Burroughs Wellcome Fund, "Program in Mathematical and Computational Neuroscience", Award Number 1001749 and by National Institutes of Health, "Rhythms of the Nervous System", Award Number 1 R01 NS46058 as part of the NSF/NIH Collaborative Research in Computational Neuroscience Program.

## References

- Adrian ED (1942) Olfactory reactions in the brain of the hedgehog. *J. Physiol.* 100: 459-473.
- Av-Ron E, Parnas H, Segel LA (1993). A basic biophysical model for bursting neurons. *Biol Cybern.* 69(1): 87-95.
- Bazhenov M, Stopfer M, Rabinovich M, Huerta R, Abarbanel HD, Sejnowski TJ, Laurent G (2001) Model of transient oscillatory synchronization in the locust antennal lobe. *Neuron* 30(2): 553-567
- Bazhenov M, Stopfer M, Rabinovich M, Abarbanel HD, Sejnowski TJ, Laurent G (2001) Model of cellular and network mechanisms for odor-evoked temporal patterning in the locust antennal lobe. *Neuron* 30(2): 569-581
- Borgers C, Kopell N (2003) Synchronization in networks of excitatory and inhibitory neurons with sparse, random connectivity. *Neural. Comput.* 3: 509-38.
- Bressler SL, Freeman WJ (1980) Frequency analysis of olfactory system EEG in cat, rabbit, and rat. *Electroencephalogr. Clin. Neurophysiol.* 50: 19-24.
- Christensen TA, Lei H, Hildebrand JG (2003) Coordination of central odor representations through transient, non-oscillatory synchronization of glomerular output neurons. *Proc. Natl. Acad Sci. U. S. A.* 100(19): 11076-81.
- Christensen TA, Waldrop BR, Hildebrand JG (1998) GABAergic mechanisms that shape the temporal response to odors in moth olfactory projection neurons. *Ann N Y Acad Sci.* 855: 475-81.
- Christensen TA, Waldrop BR, Hildebrand JG (1998) Multitasking in the Olfactory System: Context-Dependent Responses to Odors Reveal Dual GABA-Regulated Coding Mechanisms in Single Olfactory Projection Neurons. *J Neurosci.* 18(15): 5999-6008.
- Davison AP, Feng J, Brown D (2003) Dendrodendritic inhibition and simulated odor responses in a detailed olfactory bulb network model. *J. Neurophysiol.* 90(3): 21-35.
- de Bruyne M, Foster K, Carlson JR (2001) Odor coding in the *Drosophila* antenna. *Neuron.* 30(2): 537-52.
- Ermentrout B, Flores J, Gelperin A (1998) Minimal model of oscillations and waves in the *Limax* olfactory lobe with tests of the model's predictive power. *J. Neurophysiol.* 79(5): 2677-89.
- Friedrich RW, Laurent G (2001) Dynamic optimization of odor representations by slow temporal patterning of mitral cell activity. *Science* 291: 889-894.

Grunewald B (2003) Differential expression of voltage-sensitive K<sup>+</sup> and Ca<sup>2+</sup> currents in neurons of the honeybee olfactory pathway. *J Exp Biol.* 206(Pt 1): 117-29.

Hansson BS, Anton S (2000) Function and morphology of the antennal lobe: New Developments. *Annu. Rev. Entomol.* 45: 203–231.

Heinbockel T, Kloppenburg P, Hildebrand JG (1998) Pheromone-evoked potentials and oscillations in the antennal lobes of the sphinx moth *Manduca sexta*. *J Comp. Physiol. [A]*. 182(6): 703-14.

Hinds JW, Hinds PL (1976) Synapse formation in the mouse olfactory bulb. II. Morphogenesis. *J. Comp. Neurol.* 169(1): 41-61.

Hodgkin AL, Huxley AF (1952) A quantitative description of membrane current and its application to conduction and excitation in nerve. *J. Physiol.* 117(4): 500-44.

Kay LM (2003) Two species of gamma oscillations in the olfactory bulb: dependence on behavioral state and synaptic interactions. *J. Integr. Neurosci.* 2(1): 31-44.

Kay LM (2004) Two minds about odors. *Proc. Natl. Acad. Sci. U. S. A.* 101(51): 17569-70.

Kopell N, Ermentrout GB, Whittington MA, Traub RD. (2000) Gamma rhythms and beta rhythms have different synchronization properties. *Proc. Natl. Acad. Sci. U. S. A.* 97(4):1867-72.

Hoskins RF (1979) *Generalised functions*, Ellis Horwood Series: Mathematics and its applications, John Wiley & Sons.

Laurent G (1996) Dynamical representation of odors by oscillating and evolving neural assemblies. *Trends. Neurosci.* 19: 489-496.

Laurent G (2002) Olfactory network dynamics and the coding of multidimensional signals. *Nat. Rev. Neurosci.* 3(11): 884-95.

Laurent G, Davidowitz H (1994) Encoding of olfactory information with oscillating neural assemblies. *Science* 265: 1872–1875.

Laurent G, Naraghi M (1994) Odorant-induced oscillations in the mushroom bodies of the locust. *J Neurosci.* 14(5 Pt 2): 2993-3004.

Laurent G, Stopfer M, Friedrich RW, Rabinovich MI, Volkovskii A, Abarbanel HD (2001) Odor encoding as an active, dynamical process: experiments, computation, and theory. *Annu. Rev. Neurosci.* 24: 263-297.

Laurent G, Wehr M, Davidowitz H (1996) Temporal representations of odors in an olfactory network. *J. Neurosci.* 16: 3837–3847.

Leitch B, Laurent G (1996) GABAergic synapses in the antennal lobe and mushroom body of the locust olfactory system. *J. Comp. Neurol.* 372(4): 487-514.

MacLeod K, Backer A, Laurent G (1998) Who reads temporal information contained across synchronized and oscillatory spike trains? *Nature* 395: 693–697.

MacLeod K, Laurent G (1996) Distinct mechanisms for synchronization and temporal patterning of odor-encoding neural assemblies. *Science* 274: 976–979.

Mercer AR, Hildebrand JG (2002) Developmental changes in the electrophysiological properties and response characteristics of *Manduca* antennal-lobe neurons. *J. Neurophysiol.* 87(6): 2650-63.

Mercer AR, Hildebrand JG (2002) Developmental changes in the density of ionic currents in antennal-lobe neurons of the sphinx moth, *Manduca sexta*. *J. Neurophysiol.* 87(6): 2664-75.

Sachse S, Galizia CG (2002) Role of inhibition for temporal and spatial odor representation in olfactory output neurons: a calcium imaging study. *J Neurophysiol.* 87(2): 1106-17.

Shields VD, Hildebrand JG (2001) Responses of a population of antennal olfactory receptor cells in the female moth *Manduca sexta* to plant-associated volatile organic compounds. *J. Comp. Physiol. [A]*. 186(12): 1135-51.

Sivan E, Kopell N (2004) Mechanism and circuitry for clustering and fine discrimination of odors in insects. *Proc. Natl. Acad. Sci. U. S. A.* 101(51): 17861-6.

Stopfer M, Bhagavan S, Smith BH, Laurent G (1997) Impaired odour discrimination on desynchronization of odour-encoding neural assemblies. *Nature* 390: 70–74.

Stopfer M, Jayaraman V, Laurent G (2003) Intensity versus Identity Coding in an Olfactory System. *Neuron* 39: 991-1004.

Tiesinga PH, Fellous JM, Jose JV, Sejnowski TJ (2001) Computational model of carbachol-induced delta, theta, and gamma oscillations in the hippocampus. *Hippocampus.* 11(3): 251-74.

Traub RD, Miles R (1991) *Neuronal Networks of the Hippocampus*. Cambridge: Cambridge University Press.

Traub RD, Whittington MA, Colling SB, Buzsaki G, Jefferys JG (1996) Analysis of gamma rhythms in the rat hippocampus in vitro and in vivo. *J Physiol.* 493 ( Pt 2): 471-84.

Wang XJ, Buzsaki G (1996) Gamma oscillation by synaptic inhibition in a hippocampal interneuronal network model. *J Neurosci.* 16(20): 6402-13.

Wehr M, Laurent G (1996) Odor encoding by temporal sequences of firing in oscillating neural assemblies. *Nature* 384: 162–166.

Wehr M, Laurent G (1999) Relationship between afferent and central temporal patterns in the locust olfactory system. *J. Neurosci.* 19: 381–390.

Whittington MA, Traub RD, Kopell N, Ermentrout B, Buhl EH (2000) Inhibition-based rhythms: experimental and mathematical observations on network dynamics. *Int. J. Psychophysiol.* 38(3): 315-36.

Wilson DA, Stevenson RJ (2003) Olfactory perceptual learning: the critical role of memory in odor discrimination. *Neurosci. Biobehav. Rev.* 27(4): 307-28.

## Figure Legends

Figure 1. Slow patterning in 10 different PNs (out of the 14 simulated PNs, see Methods). The grey area indicates the 1 sec odor presentation. Each line represents the activity of a PN at a different trial where each dot represents an action potential fired by that PN. The reduced activity in PN 12 during odor presentation is because it is connected to a glomerulus that is inhibited by the odor (see Methods).

Figure 2: The LFP generated during odor presentation. A. The LFP (generated from the 7<sup>th</sup> trial of the simulation) filtered to frequencies between 5 Hz and 60 Hz. B. The power spectrum of the LFP seen in (A) (truncated between 2 Hz and 120 Hz). C. The power spectrum of the LFP generated from a trial where the inhibition was blocked (see text for details).

Figure 3. The effect of LN inhibition. The activity of each PN is given in 20 different trials where the first 10 trials (lower stripe, below the dividing line) describe the PN activity with LN inhibition (as in Fig. 1) and the last 10 trials (upper stripe, above the dividing line) describe the PN activity without LN inhibition.

Figure 4. Close-up on PN 9 activity in two trials: A. The PN membrane potential in a trial where the PN was connected to the network. B. The PN membrane potential in a trial where the inhibition was blocked and thus the PN was isolated. C. The ORN input to the PN in the same isolated trial as in (B) represented by the changes in the accumulative conductances of all its connected ORN synapses during the simulation. C. The internal calcium concentration in the PN in the same isolated trial as in (B).

Figure 5. Difference in firing probabilities of the various PNs at the two network configurations. The firing probability of each PN was computed for 100 ms bins ( $\sim$  twice the LFP oscillation cycle) along the two seconds of simulation after the odor is presented (10 trials for each configuration). The upper row shows the firing probability in the first network configuration where the PNs received inhibition from the LNs; the left column shows the firing probability calculated in the second network configuration where the inhibition was blocked (a prime is added to each PN to indicate the fact that it is in a stand alone configuration; e.g., PN 9'). The graphs in the table itself show the absolute difference between these probabilities, i.e., a bin by bin comparison of the activity of each PN in the first network configuration with the activity of all PNs (including its own activity) in the second. **Inset:** Hierarchical clustering of the 20 firing histograms. The first order clusters pair the histograms of each PN for each of the two network configurations; the asterisk marks the only exception.

Figure 6. Slow patterning in a spiking LN model. We changed the LN parameters so it will generate action potentials. To do so we changed the following parameters:  $g_K = 20 \mu\text{S}$ ,  $g_{Ca} = 0.0 \mu\text{S}$ ,  $g_{Na} = 9.15 \mu\text{S}$ ,  $g_{KCa} = 0.3 \mu\text{S}$ , and  $g_L = 0.3 \mu\text{S}$ . In addition we changed the description of the LN synapses onto the PNs and the other LNs to be non-graded, using Eq. 8 rather than Eq. 9 (see Appendix), and set  $g_{Inh} = 0.2 \mu\text{S}$  for LN synapses onto LNs and  $g_{Inh} = 0.4$  for LN synapses onto PNs,  $\alpha_{Inh} = 15 \text{ ms}^{-1}$  and  $\beta_{Inh} = 0.25 \text{ ms}^{-1}$ . A. The effect of LN inhibition (same as in Fig. 3 only for the varied model). B. The power spectrum of the LFP generated during odor presentation (filtered to frequencies between 5 Hz and 60 Hz). Left panel: The power spectrum in an intact network

trial. Right panel: The power spectrum of the LFP generated from a trial where the inhibition was blocked.

Figure 7. Multiphasic behavior of the PNs. To reproduce the multiphasic behavior seen in the PNs of moths (see Fig. 1 in [Christensen et al., 2003](#)) we synchronized the activity of the ORN onto the network used in Fig. 6 by setting *introduction\_rate* = 150 ms *removal\_rate* = 300 ms in all glomeruli. We increased the excited ORN *firing\_rate* to 350 Hz. We also set the odor presentation to be 500 ms (represented by the grey area). A. the LFP superimposed on top of the activity of one PN in the network. Notice the initial phase in the LFP characterized by high amplitude, followed by apparent oscillations that continues as long as the odor presentation continues. B. Close-up on the spiking activity and the LFP at two different intervals (action potentials are clipped). Notice the slower LFP at the earlier interval as observed by Christensen et al., ([2003](#)). C. the power spectrum of the LFP shows a peak around 50 Hz, even though the firing rate of each PN is much higher, and there is no obvious locking to the LFP.

Figure 8. The LN redistributes the PN action potentials. A. The membrane potential of PN 11 in a stand-alone trial (where the inhibition was blocked). B. The membrane potential of PN 11 in a trial where the network was intact.

## Appendix: Interneurons model

For the PNs and LNs we considered a single compartment model that included voltage- and calcium-dependent currents described by Hodgkin-Huxley kinetics ([1952](#)):

The voltage,  $V$ , is described by,

$$C_m \frac{dV}{dt} = I_{app} - (I_{Na} + I_K + I_{Ca} + I_{Kca} + I_L + I_{Exc} + I_{Inh}) \quad (2)$$

The sodium current,  $I_{Na}$ , potassium current,  $I_K$ , calcium current,  $I_C$ , and calcium-dependent potassium channels,  $I_{Kca}$ , are described by the general equation

$$I_x = g_x m_x^{M_x} h_x^{N_x} (V - V_x), \quad x = Na, K, Ca, Kca. \quad (3)$$

For  $I_{Na}$ :  $M_{Na} = 3$ ,  $N_{Na} = 1$ ,  $V_{Na} = 50$  mV and  $g_{Na} = 9.15$   $\mu$ S for PNs and  $g_{Na} = 1.0$   $\mu$ S for LNs.

For  $I_K$ :  $M_K$  is 4,  $N_K = 1$ ,  $V_K = -95$  mV and  $g_K = 10$   $\mu$ S for PNs and  $g_K = 3.43$   $\mu$ S for LNs;

For  $I_{Ca}$ :  $M_{Ca} = 2$ ,  $N_{Ca} = 1$ ,  $V_{Ca} = 140$  mV and  $g_{Ca} = 0.1$   $\mu$ S for PNs and  $g_{Ca} = 1.0$   $\mu$ S for LNs;

For  $I_{Kca}$ :  $M_{Kca} = 1$ ,  $N_{Kca} = 0$ ,  $V_{Kca} = -95$  mV and  $g_{Kca} = 2$   $\mu$ S;

The gating variables  $m_x(t)$  and  $h_x(t)$  satisfy,

$$\frac{dm_x}{dt} = (m_x^\infty(V) - m_x) / \tau_{m_x}(V), \quad \frac{dh_x}{dt} = (h_x^\infty(V) - h_x) / \tau_{h_x}(V). \quad (4)$$

For  $m_{Na}$ ,  $h_{Na}$ ,  $m_K$ , and  $h_K$ :

$$m_x^\infty(V) = \frac{\alpha_{m_x}(V - V_r)}{\alpha_{m_x}(V - V_r) + \beta_{m_x}(V - V_r)}, \quad \tau_{m_x}(V) = \frac{1}{\alpha_{m_x}(V - V_r) + \beta_{m_x}(V - V_r)},$$

$$h_x^\infty(V) = \frac{\alpha_{h_x}(V - V_r)}{\alpha_{h_x}(V - V_r) + \beta_{h_x}(V - V_r)}, \quad \tau_{h_x}(V) = \frac{1}{\alpha_{h_x}(V - V_r) + \beta_{h_x}(V - V_r)}, \quad x \in \{Na, K\}$$

where  $V_r = -65$  mV and  $\alpha_{m_x}$ ,  $\beta_{m_x}$ ,  $\alpha_{h_x}$  and  $\beta_{h_x}$  are taken from Traub and Miles ([1991](#)):

$$\alpha_{m_{Na}}(V) = 0.32 * (13 - V) / (e^{(13-V)^4} - 1), \beta_{m_{Na}}(V) = 0.28 * (V - 40) / (e^{(V-40)^5} - 1),$$

$$\alpha_{h_{Na}}(V) = 0.128 * e^{(17-V)/18}, \beta_{h_{Na}}(V) = 4 / (e^{(40-V)^5} + 1).$$

$$\alpha_{m_K}(V) = 0.032 * (15 - V) / (e^{(15-V)^5} - 1), \beta_{m_K}(V) = 0.5 * e^{(10-V)/40},$$

$$\alpha_{h_K}(V) = 0.028 * e^{(15-V)/15} + 2 / (e^{(85-V)^a} + 1), \beta_{h_K}(V) = b / (e^{(c-V)^{10}} + 1).$$

( $a=10$ ,  $b=0.4$  and  $c=40$  for LNs and  $a=2$ ,  $b=0.5$  and  $c=30$  for PNs)

For  $m_{Ca}$ , and  $h_{Ca}$ :

$$m_{Ca}^{\infty}(V) = \frac{1}{1 + e^{-(V+20)/6.5}}, \tau_{m_{Ca}}(V) = 10 + (V + 30) * 0.014,$$

$$h_{Ca}(V) = \frac{1}{1 + e^{(V+25)/12}}, \tau_{h_{Ca}}(V) = 0.3 * e^{(V-40)/13} + 0.002 * e^{-(V-60)/29}.$$

For  $m_{Kca}$ :

$$m_{Kca}^{\infty}(V) = \frac{[Ca]}{[Ca] + 0.025}, \tau_{m_{Kca}}(V) = \frac{100}{[Ca] + 2.525}.$$

$I_L$  is described by,

$$I_L(V) = g_L(V - V_L),$$

where  $V_L = -55$  mV and  $g_L = 0.3$   $\mu$ S for PNs and  $g_L = 0.00572$   $\mu$ S for LNs.

The calcium dynamics are described by,

$$\frac{d[Ca]}{dt} = -A * I_{Ca} - \frac{[Ca] - Ca^{\infty}}{\tau_{Ca}} \quad (5)$$

where  $Ca^{\infty}$  is  $2.4 \cdot 10^{-4}$  mM,  $A = 2 \cdot 10^{-4}$  mM $\cdot$ cm<sup>2</sup>/(ms $\cdot$  $\mu$ A) and  $\tau_{Ca} = 350$  ms in PNs and  $\tau_{Ca} = 30$  ms in LNs.

$I_{app}$  represents the applied current or external drive, and the synaptic currents  $I_{Exc}$  and  $I_{Inh}$  are described below.

### Synaptic model

The current from excitatory synapses,  $I_{Exc}$ , and the current from inhibitory synapses,  $I_{Inh}$ , following Bazhenov et al. ([2001a](#); [2001b](#)), are described by the general equation

$$I_{Syn} = g_{Syn} [O]_{Syn} (V - V_{Syn}), \quad Syn = Exc, Inh. \quad (6)$$

Where  $[O]_{Syn}$ , the fraction of open channels, is described by,

$$\frac{d[O]_{Syn}}{dt} = \alpha_{Syn}(1 - [O]_{Syn})[T]_{Syn} - \beta_{Syn}[O]_{Syn}. \quad (7)$$

For  $I_{Exc}$ ,  $V_{Exc} = 0$  mV and  $g_{Exc} = 0.0006$   $\mu$ S for ORN synapses onto LNs,  $g_{Exc} = 0.005$   $\mu$ S for synapses onto PNs and  $g_{Exc} = 0.04$   $\mu$ S for PN synapses onto LNs.  $\alpha_{Exc} = 10$   $ms^{-1}$  and  $\beta_{Exc} = 0.16$   $ms^{-1}$  for ORN synapses and  $\beta_{Exc} = 0.2$   $ms^{-1}$  for PN synapses;  $[T]_{Exc}$  is described by,

$$[T]_{Exc}(t) = 0.5\theta((t_0 + Delay) + t_{max} - t)\theta - (t_0 + Delay), \quad (8)$$

where  $\theta(t)$  is the Heaviside step-function ([Hoskins, 1979](#)),  $t_{max} = 0.3$  ms,  $t_0$  is the time of the action potential's pick in the pre-synaptic neuron and the synaptic delay,  $Delay$ , is 2 ms.

For  $I_{Inh}$ ,  $V_{Inh} = -70$  mV and  $g_{Inh} = 3$  mS for synapses between LNs and LNs and  $g_{Inh} = 3.5$  mS for synapses between LNs and PNs.  $\alpha_{Inh} = 15$   $ms^{-1}$  and  $\beta_{Inh} = 0.25$   $ms^{-1}$ ;  $[T]_{Inh}$  is described by,

$$[T]_{Inh}(t) = \frac{1}{1 + e^{(-V_{Pre}(t-Delay) - V_0)/\sigma}}, \quad (9)$$

where  $V_0 = -20$  mV,  $\sigma = 1.5$ ,  $V_{Pre}(t)$  is the voltage of the pre-synaptic neuron and the synaptic delay,  $Delay$ , is 2 ms.

Figure 1  
[Click here to download Figure: Figure 1.ppt](#)

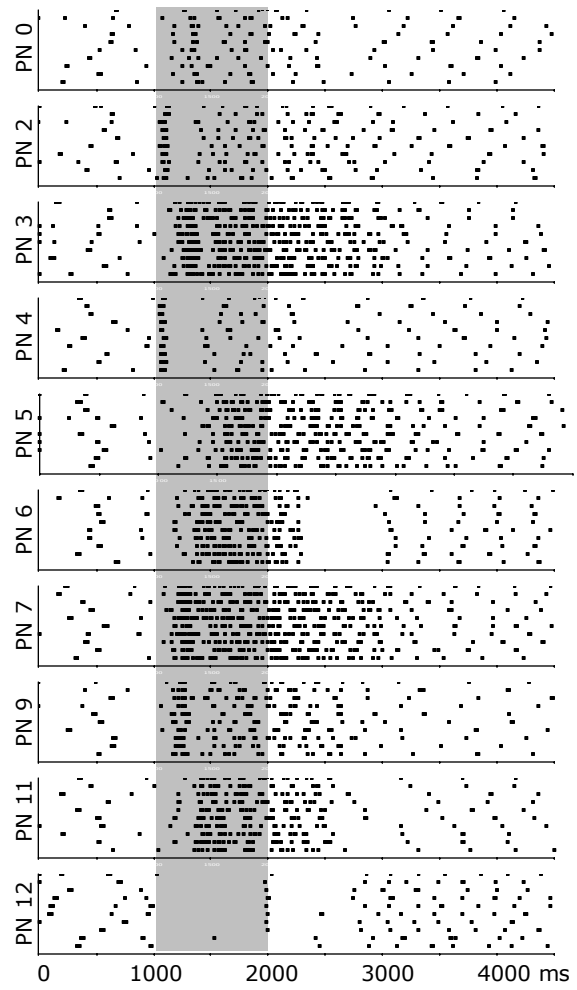


Figure 2

[Click here to download Figure: Figure 2.ppt](#)

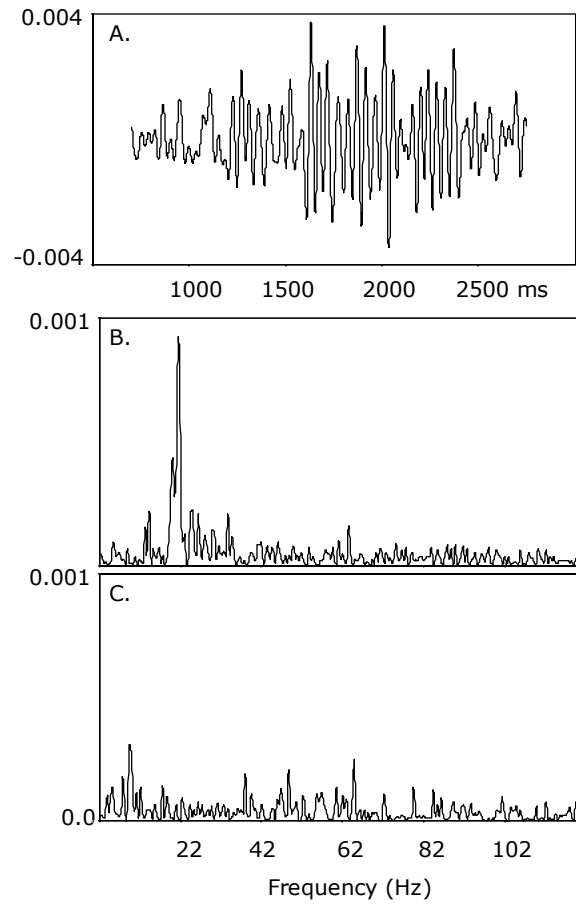
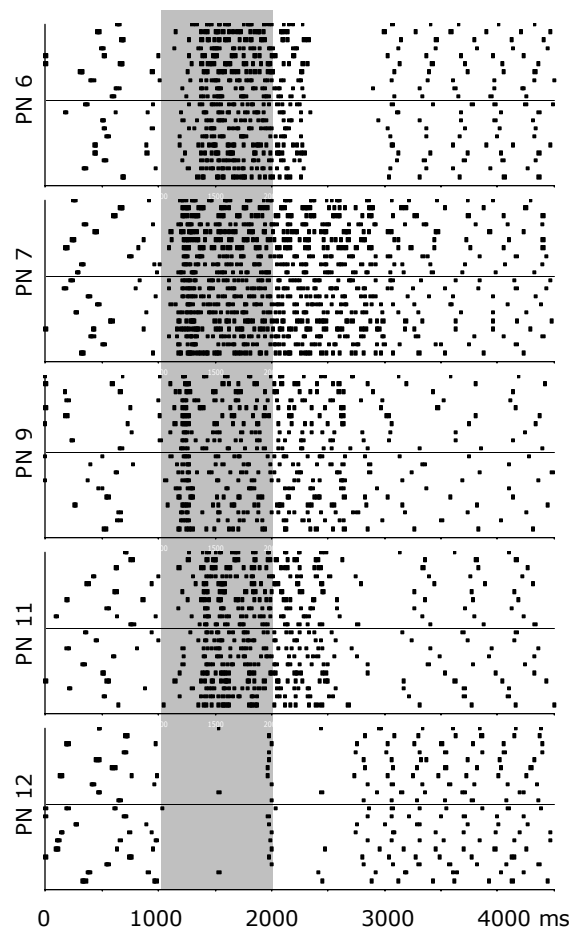
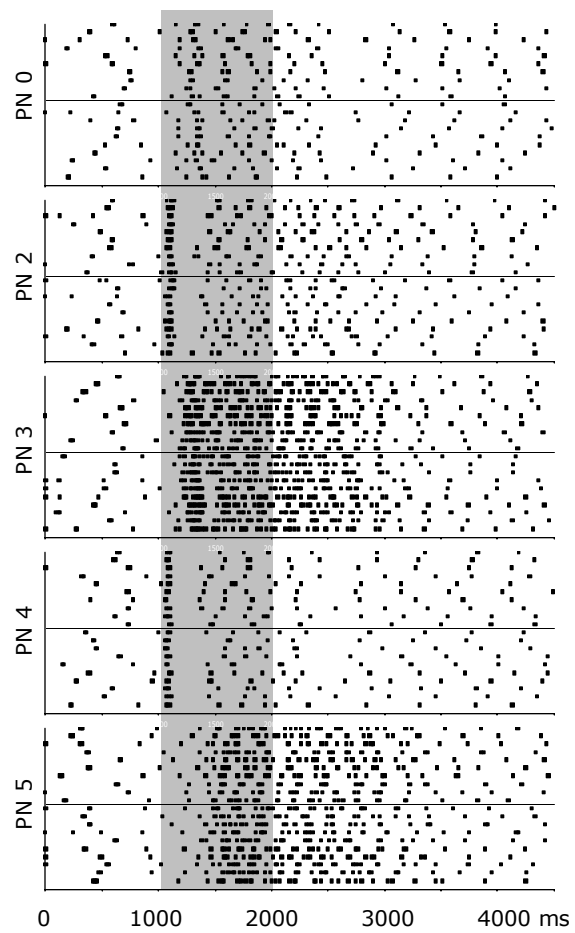
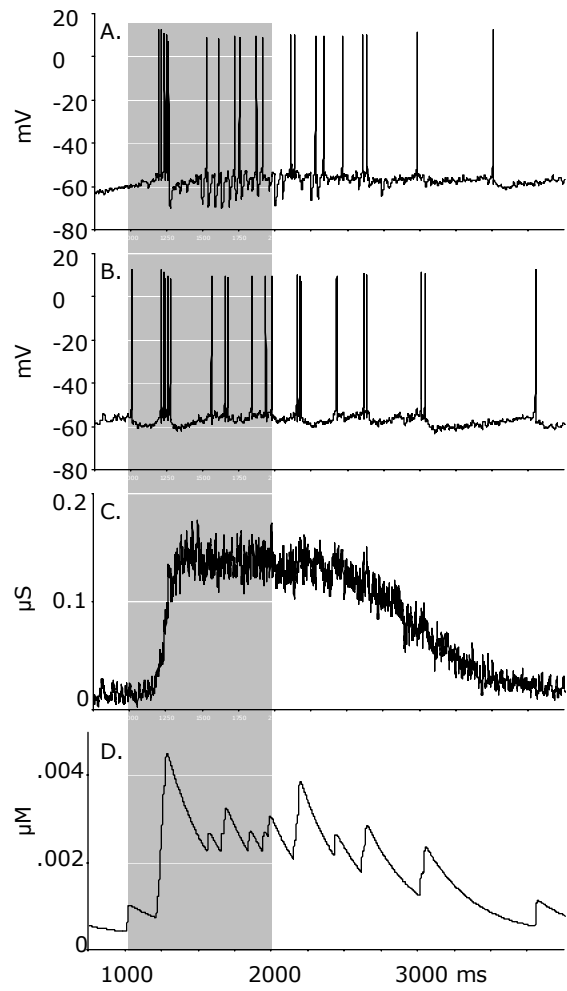


Figure 3, Two columns

[Click here to download Figure: Figure 3 - Two columns.ppt](#)



**Figure 4**  
[Click here to download Figure: Figure 4.ppt](#)



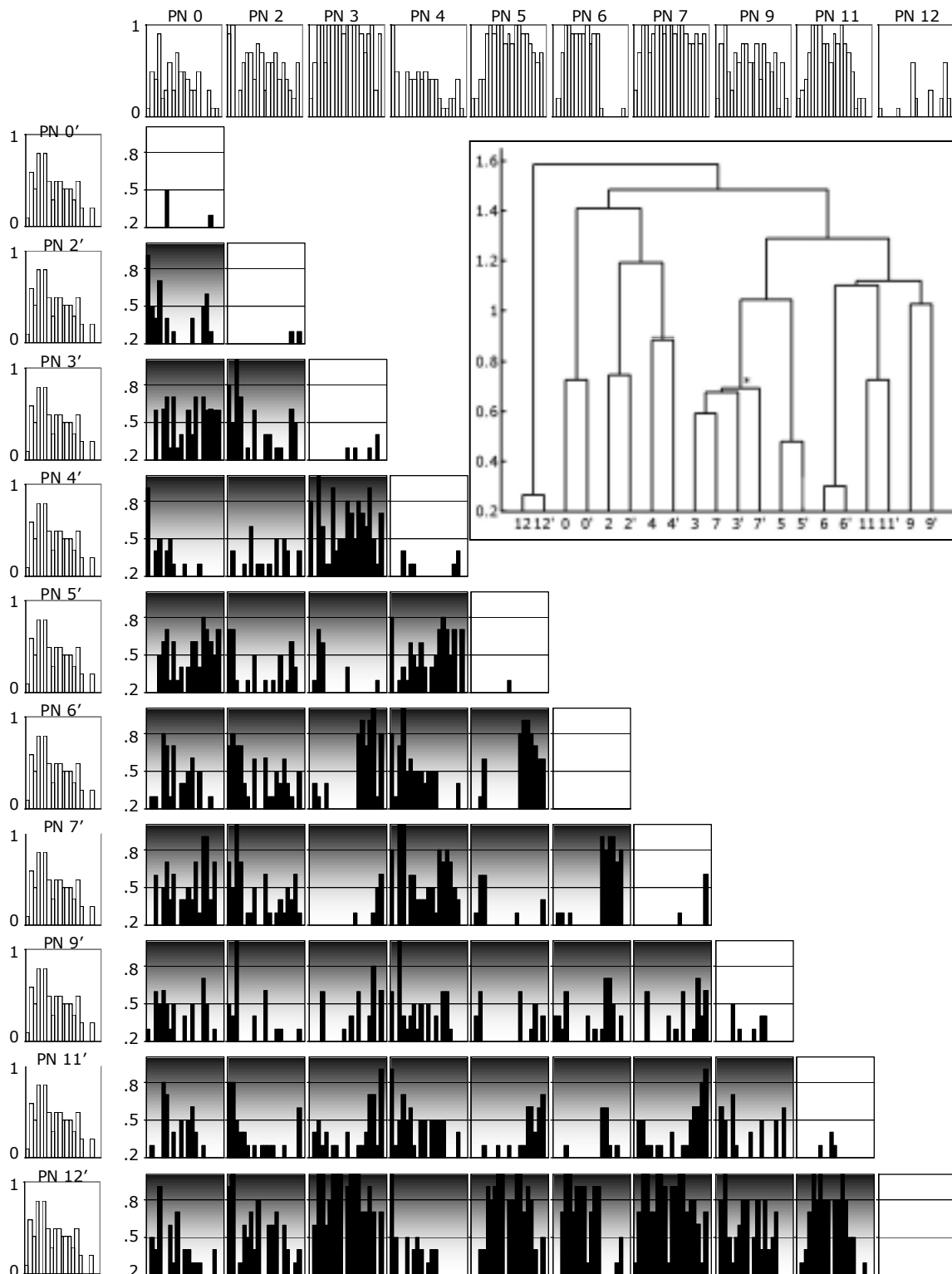
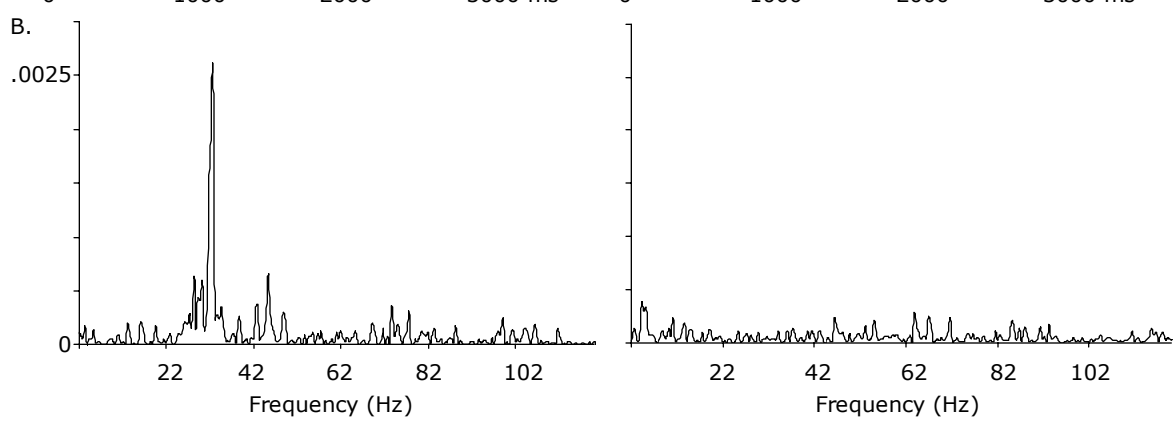
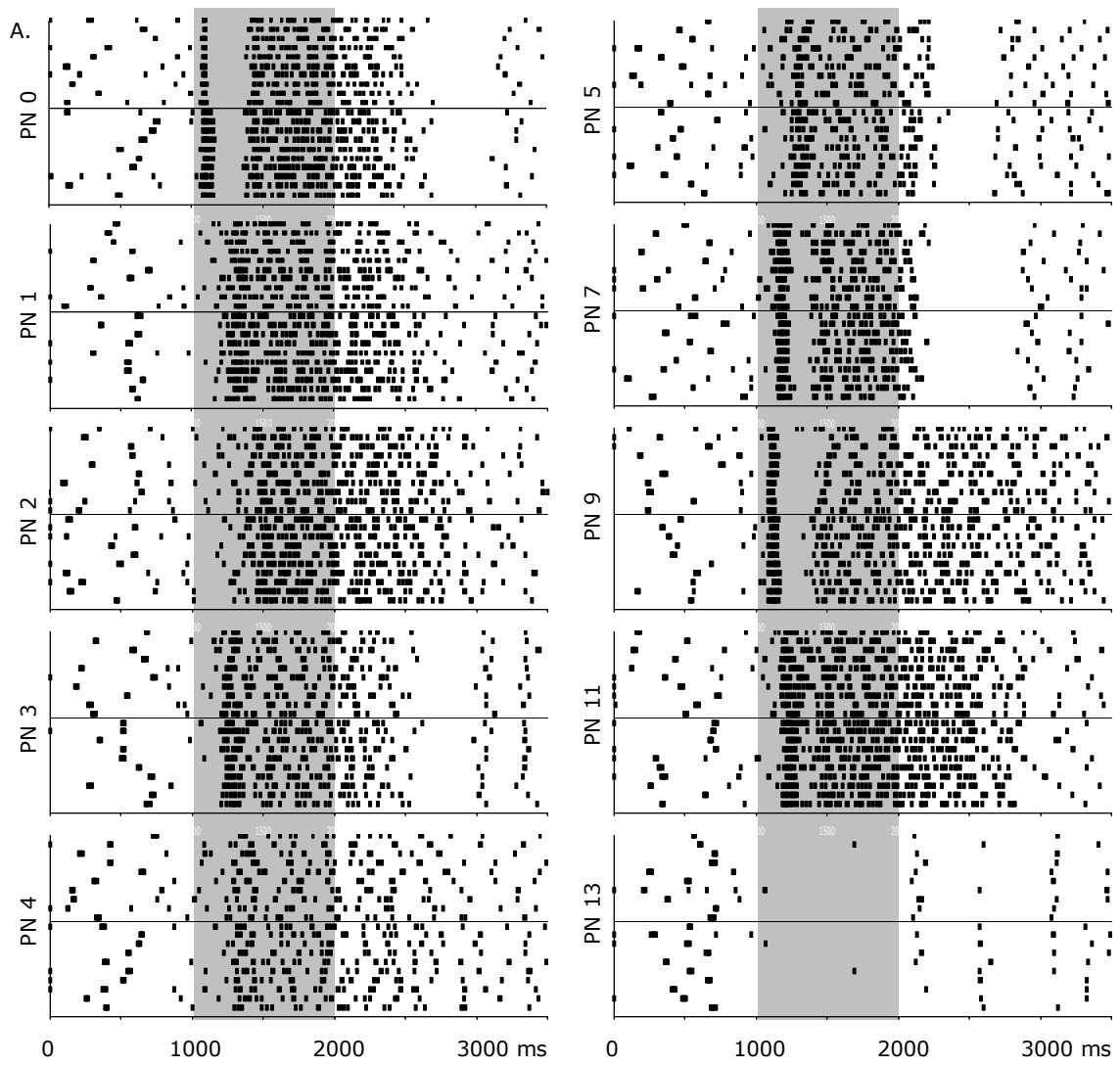
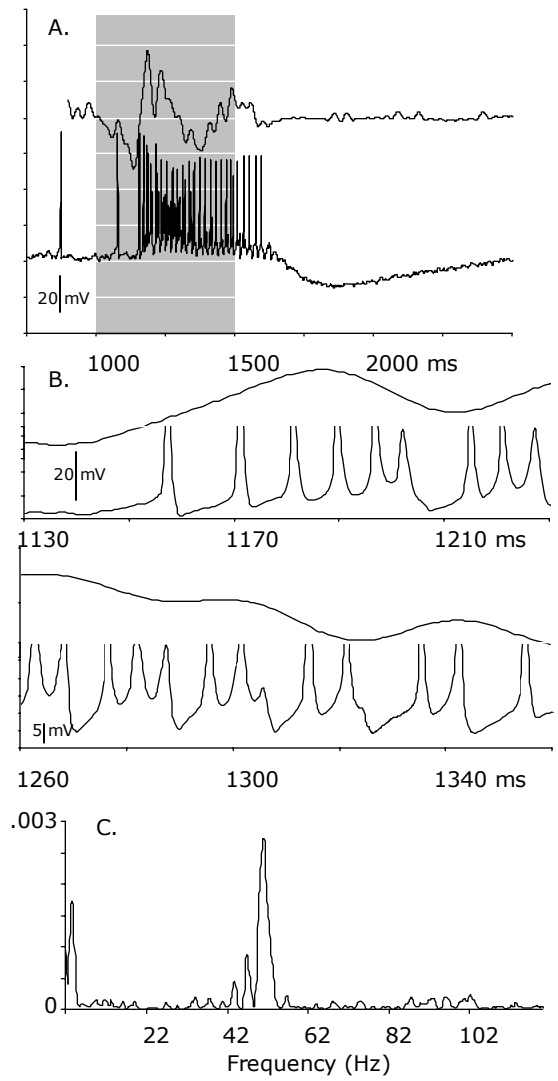


Figure 6, Two columns  
[Click here to download Figure: Figure 6 - Two columns.ppt](#)



**Figure 7**  
[Click here to download Figure: Figure 7.ppt](#)



**Figure 8**  
[Click here to download Figure: Figure 8.ppt](#)

